JB Accepted Manuscript Posted Online 11 April 2016
J. Bacteriol. doi:10.1128/JB.00020-16

Azospirillum brasilense chemotaxis depends on two signaling pathways regulating distinct motility parameters

Tanmoy Mukherjee[1], Dhivya Kumar[1*], Nathan Burriss[1], Zhihong Xie[1, 2] and Gladys Alexandre[1]†

[1]Department of Biochemistry, Cellular and Molecular Biology, The University of Tennessee, Knoxville, TN 37996, USA

[2]Yantai Institute of Coastal Zone Research, *Chinese* Academy of Sciences, Yantai, Shandong, P. R. China

Running title: Chemotaxis signal transduction in *Azospirillum*

Key words: *Azospirillum*, chemotaxis, motility, rhizosphere, speed

†To whom correspondence should be addressed:
Department of Biochemistry, Cellular and Molecular Biology, The University of Tennessee, Knoxville, TN 37996; Phone: 865-974-0866; Fax: 865-974-6306; Email: galexan2@utk.edu

* Present address: Department of Molecular Biology and Biophysics, University of Connecticut Health Center, Farmington, CT 06030

ABSTRACT

The genomes of most motile bacteria encode two or more chemotaxis (Che) systems but their functions have been characterized in only a handful of model systems. *Azospirillum brasilense* is a motile soil alphaproteobacteria able to colonize the rhizosphere of cereals. In response to an attractant, motile *A. brasilense* cells transiently increase swimming speed and suppress reversals. The Che1 chemotaxis pathway was previously shown to regulate changes in the swimming speed but it has a minor role in chemotaxis and root surface colonization. Here, we show that a second chemotaxis system, named Che4, regulates the probability of swimming reversals and is the major signaling pathway for chemotaxis and wheat root surface colonization. Experimental evidence indicates that Che1 and Che4 are functionally linked to coordinate changes in the swimming motility pattern in response to attractants. The effect of Che1 on swimming speed is shown to enhance the aerotactic response of *A. brasilense* in gradients, likely providing the cells with a competitive advantage in the rhizosphere. Together, the results illustrate a novel mechanism by which motile bacteria utilize two chemotaxis pathways regulating distinct motility parameters to alter movement in gradients and enhance the chemotactic advantage.

IMPORTANCE Chemotaxis provides motile bacteria with a competitive advantage in the colonization of diverse niches and is a function enriched in rhizosphere bacterial communities, with most species possessing at least two chemotaxis systems. Here, we identify the mechanism by which cells may derive a significant chemotactic advantage using two chemotaxis pathways that ultimately regulate distinct motility parameters.

INTRODUCTION

Bacterial chemotaxis provides a competitive advantage by guiding motile cells in gradients of chemoeffectors toward environments that support growth and metabolism. Chemotaxis contributes to the establishment of various associations of bacteria with eukaryotic hosts (mammals, insects, and plants) and promotes virulence, symbiosis and the establishment of microbial communities (1). Bacterial chemotaxis and motility are widespread traits encoded in the genomes of bacteria inhabiting diverse environments and these functions are specifically enriched in microorganisms found in soils (2), suggesting that they provide a significant competitive advantage in this environment. Consistent with these findings, comparative genome analyses of chemotaxis in diverse motile bacteria suggested that most bacteria possess two chemotaxis systems and soil–dwelling bacteria have often more than two chemotaxis systems (3).

The molecular mechanism of chemotaxis signal transduction has been deciphered in most detail in the model organism, *Escherichia coli*, which possesses a single chemotaxis system. In *E. coli*, the chemotaxis signal transduction pathway consists of membrane bound receptors clustered in dense arrays at the cell poles where their C-terminal domains associate with cytoplasmic CheA kinase and the CheW scaffolding protein. When stimulated by a repellent, CheA autophosphorylates on a conserved histidine residue (H48) using ATP and transfers its phosphate to the aspartate residue (D57) of CheY (1). Phospho-CheY binding to flagella motors with high affinity triggers a switch in the direction of flagella motor rotation from counterclockwise to clockwise. This event causes a change in the swimming direction of the cell, or a tumble (1). A

phosphatase, CheZ assists signal termination by acting on phospho-CheY (1). In addition, a receptor-specific methyltransferase, CheR and a receptor-specific methylesterase CheB activated by phosphotransfer from phospho-CheA, differentially methylate the receptors to reset sensitivity (1). This basic set of chemotaxis proteins comprises a signaling pathway that is generally conserved across bacterial species (3). However, there are notable exceptions to this paradigm such as the absence of CheB and CheR in some species, the existence of multiple CheY response regulators in others or the presence of ancillary chemotaxis proteins not found in *E. coli* (1). Another variation on this theme is the presence of multiple chemotaxis pathways in the genome of most motile bacteria (3). Some of these additional chemotaxis pathways regulate type IV pili-dependent motility or alternative cellular functions (ACF) and they can be identified due to their unique structure (3). Most chemotaxis pathways found in bacterial genomes are predicted to regulate flagellar motility patterns. The contribution of multiple chemotaxis systems to the regulation of changes in the swimming direction was demonstrated in some species. For example, in *Rhodobacter sphaeroides*, two chemotaxis systems together control the probability of stops in flagellar rotation (4).

Azospirillum brasilense is a motile soil bacterium that inhabits the rhizosphere of diverse plant species. *A. brasilense* cells swim using a single polar flagellum and change swimming direction when the direction of flagellar rotation briefly reverses, causing cells' movement to be re-directed in a different direction (5). In addition to regulating the probability of swimming reversals, motile *A. brasilense* cells navigating an attractant gradient can transiently increase swimming speed (6). The available genome sequence of *A. brasilense* indicates the presence of four distinct chemotaxis operons, three of which

(Che1, Che2 and Che3) are also encoded in the genomes of all *Azospirillum* strains sequenced to date as well as in the genome of the closely related *Rhodospirillum centenum* (7-10), suggesting they were present in the last common ancestor of these two genera (Fig. 1). The chemotaxis pathway that regulates transient increases in swimming speed in response to attractants has been identified as Che1 (6). The existence of a distinct pathway for controlling swimming reversals comes from the observation that inactivation of *cheB1* or *cheR1* impaired the ability to regulate the probability of swimming reversals but not mutations in either *che1*, *cheA1* or *cheY1* (11). These data were interpreted to suggest that Che1 functionally interacts with the unidentified pathway controlling the probability of swimming reversals (6). However, the chemotaxis pathway(s) responsible for controlling changes in the direction of flagellar rotation to trigger reversals is not yet known. The role of Che2 in *A. brasilense* is unknown but it is a homolog to the Che2 operon controlling flagellar biosynthesis in *R. centenum* (10). In *A. brasilense*, *che2* does not appear to be expressed under standard laboratory conditions (Xie and Alexandre, unpublished). Che3 is a chemotaxis-like ACF pathway that was recently implicated in the control of flocculation in *A. brasilense* (12).

Che4 is present in the genome of all *Azospirillum* strains sequenced to date, but absent from the *R. centenum* genome. In *R. centenum*, the Che1 chemotaxis system controls all chemotaxis responses (13) in contrast to its homolog in *A. brasilense* (Che1) that controls swimming speed and has only a minor role in chemotaxis. The Che4 system is thus the most likely candidate for controlling the probability of swimming reversals in this species. Here, we show that Che4 is essential for all chemotaxis responses in *A. brasilense* and for competitive wheat root surface colonization. We demonstrate that the

signaling output from Che4 directly modulates the probability of reversals and that signaling from Che1 and Che4 is integrated during chemotaxis to produce an enhanced response to attractants. These results illustrate a novel mechanism by which motile bacteria utilize two chemotaxis pathways regulating distinct motility parameters to alter movement in gradients and to increase their chemotactic advantage.

MATERIALS AND METHODS

Bacterial Strains and Growth Conditions. Bacterial strains used in this study are listed in Table 1. The *A. brasilense* strains were grown at 28°C with shaking (200 rpm). The MMAB (minimal medium for *A. brasilense*) medium was prepared as described previously (14, 15). Cells were induced for nitrogen fixation by first growing them in MMAB followed by three to four washes of the cell pellet in sterile chemotaxis buffer (10 mM phosphate buffer [pH 7.0], 1 mM EDTA) (11) by centrifugation. The pellet was then re-suspended in MMAB lacking any nitrogen source. Nitrogen fixation was induced by growth under these conditions overnight at 28°C and without shaking to ensure low aeration conditions. All culture stocks were routinely maintained on tryptone-yeast (TY) medium (per liter, 10 g bacto tryptone, 5 g yeast extract) or MMAB solidified with 1.5% (w/v) agar. Antibiotics for *A. brasilense* were added at the following final concentrations: ampicillin (200 µg/ml), chloramphenicol (20 µg/ml), kanamycin (30 µg/ml), gentamycin (20 µg/ml) and tetracycline (10 µg/ml).

Mutagenesis. To construct a strain deleted for the *cheA4* gene, a 843 bp upstream fragment including 126 bp of *cheA4* and a downstream 825 bp sequence including 232 bp

139 at the 3' end of *cheA4* were PCR amplified using *cheA*4Up-F, *cheA*4Up-R, *cheA*4Dwn-F
140 and *cheA4*Dwn-R (Table S1). These primers were engineered to include 5' XbaI
141 (*cheA4*Up-F) and 3'HindIII (*cheA4*Dwn-R) restriction sites for cloning into pUC19 as
142 well as BamHI sites (present at the 5' end of *cheA*4Up-R and at the 3' end of *cheA*4Dwn-
143 F) to permit subsequent insertion of a gentamycin resistance (Gm^r) cassette isolated from
144 p34S-Gm by BamHI restriction digestion (Table 1). After verification by sequencing, the
145 Δ*cheA4*::Gm^r region present on the pUC19 vector was isolated by restriction digestion
146 with XbaI and HindIII and inserted into the suicide vector pSUP202 (Table 1), digested
147 with the same enzymes, yielding pSUPΔ*cheA4*::Gm^r. The pSUPΔ*cheA4*::Gm^r vector was
148 transformed into *E.coli* S17-1 for biparental mating with strains *A. brasilense* Sp7 and its
149 Δ*cheA1* mutant derivative for allelic exchange, as previously described (15). For
150 constructing a mutant lacking *cheY4*, an upstream fragment encompassing the first 6 bp
151 of *cheY4* and an additional 577 bp of upstream DNA sequence as well as a downstream
152 fragment including the last bp of *cheY4* and an additional 584 bp downstream of the stop
153 codon were amplified using the primer pair *cheY4*Up-F and *cheY4*Up-R and *cheY4*Dwn-F
154 and *cheY4*Dwn-R (Table S1) which were designed to include restriction sites to facilitate
155 cloning into EcoRI and HindIII digested pUC19 vector. The fragments were also
156 engineered to include a BamHI site for insertion of a chloramphenicol cassette isolated
157 from a p34S-Cm BamHI-digested vector. The *cheY*4 deletion insertion construct in
158 pUC19 was verified by sequencing. The sequenced verified fragment was isolated by
159 digestion with EcoRI and HindIII and cloned into the pKGmobGII suicide vector to yield
160 pKGΔ*cheY4*::Cm^r (Table 1). The latter was transformed into *E.coli* S17-1 cells and
161 transferred into *A. brasilense* Sp7 or its Δ*cheY1* mutant derivative by biparental mating

for allelic exchange, as described above. Strains carrying appropriate deletions were verified by PCR. To construct a strain deleted for most of the *che4* sequence, we first used PCR amplification of a 698 bp fragment encompassing the first gene of the *che4* cluster (Fig. 1) and upstream DNA sequence using *che4*Up-F and *che4*Up-R (Table S1) and a 722 bp fragment overlapping the last gene of *che4* (Fig. 1) and including additional downstream DNA sequence using *che4*Dwn-F and *che4*Dwn-R (Table S1). The primers *che4*Up-R and *che4*Dwn-F were designed to include 12 bp of overlapping DNA sequence that were used in a second round of SOE PCR (16) to produce a 1420 bp fusion product between the upstream and downstream PCR fragments. The 1420 bp product was restriction digested with PstI and XbaI, which were engineered in the *che4*Up-F and the *che4*Dwn-R primers, respectively (Table S1), and cloned into pUC19. The fusion construct cloned in pUC19 was further digested with SalI in order to insert a SalI-digested gentamycin resistance cassette isolated from the p34S-Gm vector (Table 1) and yield a Δ*che4*::Gm^r construct cloned in pUC19. After verification by sequencing, the Δ*che4*::Gm^r region was isolated as a PstI and XbaI fragment which was then cloned into the suicide vector pSUPPOL2SCA (17). The suicide vector carrying the *che4* deletion insertion construct was transformed into *E. coli* strain S17-1 followed by allelic exchange after transfer to *A. brasilense* wild type strain Sp7 and its Δ*che1* mutant derivative by biparental mating, as described above. Mutants carrying the correct deletion insertions were identified by PCR.

Complementation and site-specific mutations of *cheA4* and *cheY4* genes. Functional complementation of the mutant phenotypes was carried out by expressing the parental

Journal of Bacteriology

genes or mutated alleles *in trans*, from the broad host range pRK415 vector (Table 1). The genes were cloned in-frame and downstream of the plasmid-born *lac* promoter with engineered restriction sites and a ribosome binding site to ensure expression (Table 1)(6). Each gene was amplified from the genomic DNA of the wild type strain, using a set of forward and reverse primers that are listed in Table S1. The genes coding for the kinase inactive CheA4^{H54Q} and the inactive CheY4^{D57N} were synthesized by Genscript (Genscript, Piscataway, NJ) and cloned into pUC57 between EcoRI and HindIII sites. The *cheA4* and *cheY4* inserts were sub-cloned into pCR2.1 by TOPO cloning according to the manufacturer's instructions (Invitrogen, CA) for verification by sequencing, followed by digestion with EcoRI and HindIII to isolate the sequence-verified genes. The isolated DNA fragments were cloned into the pRK415 vector. Recombinant plasmids were isolated from transformed *E. coli* TOP10 cells, prior to being transferred into *E. coli* S17-1 for biparental mating with *A. brasilense* recipient strains, as described above. An empty pRK415 vector was transferred to *A. brasilense* Sp7 and its mutant derivatives to be used as controls.

Behavioral assays. For the capillary assay for aerotaxis, cells were grown to an OD_{600} of 0.4-0.6 (exponential phase of growth) in MMAB supplemented with malate (10 mM) and ammonium (18.7 mM). Cultures were adjusted to an equivalent number of cells (estimated via OD_{600} measurements) by dilution in chemotaxis buffer. The cells were gently washed three times with chemotaxis buffer by low speed centrifugation and re-suspended in 100 µl MMAB containing malate (10 mM). All cells remained motile under these conditions. Cells were transferred to an optically flat capillary tube (Vitro

Dynamics, Inc., Rockaway, N.J.) by immersing a capillary tube into the cell suspension. Aerotaxis was visualized under the light microscope as the formation of a stable band of motile cells at a distance from the air-liquid interface (meniscus). An aerotaxis band typically forms within 2-3 minutes and is stable for a minimum of 25 minutes under these conditions (18). The assay was performed in triplicate using independent cultures. Images were captured using the 4X objective of a phase contrast Nikon E200 microscope via a C-mounted Nikon Coolpix digital camera.

For chemotaxis in a spatial gradient, soft agar plates were prepared using MMAB solidified with 0.3% agar and supplemented with malate (10 mM) and ammonium chloride (18.7 mM). Cells were grown as indicated above for aerotaxis and the cell suspensions were adjusted to an equivalent number of cells, estimated by OD600 measurements, prior to being inoculated in the center of the soft agar plates. The inoculated plates were incubated at 28^{o}C for 48 hours before being photographed. The experiment was performed in triplicate for each strain.

Computerized motion tracking of free-swimming cells. Digital movies of free-swimming cells were captured using the 40X objective of a phase contrast Nikon Eclipse E200 microscope fitted with a SONY HyperHAD monochrome camera, at a rate of 30 frames per second. The videos were converted to a digital format using IC Capture2 software (The Imaging Source, Charlotte, NC) before being analyzed using CellTrak 1.5 software (Motion Analysis, Santa Rosa, CA). Changes in swimming parameters (velocity and reversal frequency) were determined on a minimum of 75 cells, recorded from at least 2 different fields of view and 3 independent cultures. Velocity is expressed as

231 micrometer per second and reversal frequency as the number of swimming reversals per
232 second and per cell.

233

234 **Plant Inoculation.** Wheat seeds (*Triticum aestivum*) were surface sterilized and
235 germinated for three days in the dark followed by an additional day in the light, as
236 previously described (19). Fifty mL of Fahraeus medium ($CaCl_2$, 100 mg l^{-1},
237 $MgSO_4.7H_20$, 120 mg l^{-1}, KH_2PO_4, 100 mg l^{-1}, Na_2HPO4, 150 mg l^{-1} and ferric citrate 5
238 mg l^{-1}) solidified with 0.6% agar was placed in a 6.5 cm diameter growth chamber. Four
239 plantlets were placed at equal distance from each other and from the center of the growth
240 chamber. Strains to be tested were inoculated at the center of the chamber. Eight
241 chambers (with four plants each) were prepared per trial, yielding a minimum of 8
242 replicates. For inoculation, strains were grown in MMAB supplemented with malate
243 (10mM) and ammonium chloride (18.7 mM) to an OD_{600} of 0.5. Two mL of the culture
244 were pelleted and washed 3 times with sterile 0.8% KCl by centrifugation and re-
245 suspended in 400 µL of sterile 0.8% KCl. Twenty µL of this suspension was inoculated
246 into the center of the growth chamber. The number of cells in the inoculum was
247 determined by CFU counts. For competitive root colonization assays, the strains to be
248 compared were prepared as indicated above and mixed in a 1:1 ratio prior to inoculation
249 into the chambers. The chambers were incubated at 25°C for 24 hours after which the
250 plants were removed and the roots excised. The roots of the four plantlets from a single
251 growth chamber were combined and homogenized in 5 mL 0.8% KCl followed byserial
252 dilutions and plating on selective media to determine CFU. Root colonization was
253 calculated as a colonization index for plants inoculated with a single strain and as a

competitive index for the plants inoculated with two strains. The colonization index for individual strain is the Log_{10} (strain output/strain input), where the number of CFU extracted from roots after incubation is normalized to the CFU measured in the inoculated input. The competitive index is a ratio calculated as follows: Log_{10} (mutant output/wild-type output)/ (mutant input/wild-type input).

Identification of chemotaxis proteins in the complete genome sequence of *A. brasilense*. The *che1* operon organization was previously described (14). To identify other chemotaxis proteins, we used the sequences of the chemotaxis homologs reported in the genome description of *A. brasilense* Sp245 (10) as queries to search the genome of *A. brasilense* Sp7 (NCBI accession: PRJNA293508) using the BLAST server (20).

Statistical analysis. For comparing wild type and mutant phenotypes (swimming speed, swimming reversals and plant colonization), we determined average values from at least three independent experiments performed in duplicates and performed one-way ANOVA (alpha level of 0.05), followed by pairwise two-sample *t*-tests assuming equal variances (alpha level 0.05) using Prism6 (GraphPad software Inc., San Diego, CA).

RESULTS

***che4* mutants lack chemotaxis and aerotaxis.** Genome sequence analysis predicted that Che4 is the major chemotaxis system in *A. brasilense*. To test this hypothesis, we constructed strains lacking *cheA4* (Δ*cheA4*, strain AB401), *cheY4* (Δ*cheY4*, strain AB402) or the entire *che4* cluster (Δ*che4*, strain AB403)(Table 1) and tested their

chemotaxis and aerotaxis abilities using spatial gradient assays (Fig. 2). All mutants were motile and grew at similar rates under various media and incubation conditions (data not shown). While the Δ*cheA4* mutant was null for chemotaxis and aerotaxis, the Δ*cheY4* and Δ*che4* mutants were null for aerotaxis but displayed residual chemotaxis in the soft agar assay (Fig. 2A and 2B). Similar patterns were observed when other carbon sources were used in the soft agar assay (data not shown). The different phenotypes of some of these mutants in chemotaxis versus aerotaxis were intriguing. The discrepancy between the behavior of the Δ*cheY4* and Δ*che4* mutants in the aerotaxis versus the chemotaxis assay could be due to the different incubation times and conditions under which these assays are conducted. The aerotaxis assay is performed using a suspension of free-swimming cells placed into a capillary tube. The aerotactic band typically forms within 2-3 minutes. The chemotaxis rings formed in soft agar plates are observed after at least 24-48 hours of growth. One possibility is that the rings observed in the soft agar plates are the result of pseudotaxis, which is a form of translocation through the agar that does not result from chemotaxis signaling; these have been reported under similar conditions in several bacterial species (21-23). The aerotaxis defects of the Δ*cheA4* and Δ*cheY4* could be complemented by expressing a parental gene from a broad host range plasmid but not by expressing a variant allele of *cheA4* or *cheY4* carrying a single mutation on the predicted phosphorylatable histidine (H54Q in CheA4) and aspartate (D57N in CheY4) residues, respectively (Fig. 2C and 2D). These data indicate that conserved phosphorylatable residues on CheY4 and CheA4 must be present for signaling to occur, suggesting that a phosphorylation cascade between CheA4 and CheY4 triggers changes in the direction of flagellar rotation to cause swimming reversals. Together, these results identify CheA4 as

300 the major histidine kinase mediating aerotaxis and chemotaxis in *A. brasilense* and they
301 further suggest that signaling from Che4 plays a major role in controlling the changes in
302 the direction of flagellar rotation during swimming reversals.
303
304 **The signaling output from Che4 is the control of the swimming reversal frequency.**
305 As indicated above, the formation of chemotaxis rings in the soft agar assay and of the
306 aerotaxis bands in the capillary assay are not identical behaviors. The ultimate signaling
307 output of a bacterial chemotaxis pathway is the control of the swimming motility pattern
308 by affecting the probability of reversals. In other words, mutants unable to chemotax are
309 expected to either constantly run or constantly reverse swimming direction. We assessed
310 the swimming motility patterns of the Δ*che4*, the Δ*cheA4* and, the Δ*cheY4* mutants under
311 steady state conditions (Fig. 3A). The wild type strain swam with long runs interrupted
312 by instances of reversals that occurred with an average probability of about 0.5 reversal/s
313 (Fig. 3B). Compared to the wild type, mutants lacking CheA4 swam in straight runs and
314 did not reverse (Fig. 3A and 3B). The Δ*cheY4* mutant had a surprisingly different
315 phenotype from the Δ*cheA4* mutant in that it also swam with fewer instances of reversals
316 compared to the wild type strain (Fig. 3A and 3B) but it clearly was still able to reverse
317 swimming direction (Fig. 3A). The strain lacking the *che4* cluster (Δ*che4*) displayed a
318 frequency of reversals that was not significantly different from that of the wild type strain
319 (0.6 reversal/s) (Fig. 3A and 3B). Analysis of free-swimming cells of the Δ*che4* strain
320 also revealed a significantly erratic ('jiggly") motility pattern (Fig. 3A). This analysis
321 thus confirms that CheA4 is essential for the cells to reverse swimming direction. The
322 lack of CheY4 or Che4 severely impaired, but did not eliminate the ability of cells to

reverse while lack of CheA4 completely abolished it, indicating that CheY4 (and thus Che4) has a major, but not unique role in this behavior.

Che1 and Che4 together contribute to regulating the swimming pattern. The distinct swimming pattern of the Δ*cheY4* and Δ*che4* strains compared to the Δ*cheA4* was unexpected since all three strains should display the same phenotype if the signaling output of the Che4 pathway is the control of swimming reversals. Che1 controls changes in swimming speed during chemotaxis and previous data have suggested that signaling from Che1 and from the pathway affecting swimming reversals functionally interacted (6, 24). Therefore, we hypothesized that Che1 may be responsible for the residual swimming reversal ability of the Δ*cheY4* and the Δ*che4* mutants. To test this possibility, we constructed strains lacking both *che1* and *che4* (Δ*che1*Δ*che4*; strain AB143), both *cheA1* and *cheA4* (Δ*cheA1*Δ*cheA4*; strain AB141) and both *cheY1* and *cheY4* (Δ*cheY1*Δ*cheY4*; strain AB142) (Table 1) and analyzed their swimming patterns (Fig. 3C). We found that mutating *cheY1* and *che1* in the Δ*cheY4* and Δ*che4* mutant backgrounds yielded cells unable to reverse swimming direction, similar to the motility pattern observed for the Δ*cheA4* strain or, as expected, for the Δ*cheA1*Δ*cheA4* strain (Fig. 3B and 3C). Disabling Che1 in the Δ*che4* mutant (strain AB143) background also abolished the erratic swimming behavior of the Δ*che4* strain, suggesting that signaling from Che1 caused this behavior (Fig. 3B and 3C). The Δ*che1*Δ*che4* mutant strain and, to a lesser extent, the Δ*cheA1*Δ*cheA4 strain* also persisted and swam in circles close to the surface of the coverslip (Fig. 3C). This behavior has been associated with smooth swimming close to surfaces in *E. coli* (25, 26) and is thus consistent with the lack of swimming reversals in

these strains. However, we do not know why this behavior is more preeminent in these two mutants but not in the Δ*cheY1*Δ*cheY4* strain. Since Che1 affects the swimming speed, we also analyzed this motility parameter for mutants lacking *che4* genes alone or in combination with mutations in *che1* genes. We found that only the Δ*cheA4* and the Δ*che4* mutants had a small, but significant, reduction in steady-state swimming speed compared to the wild type strain (Fig. 3B). This phenotype was absent in the Δ*cheA1*Δ*cheA4* and Δ*che1*Δ*che4* strains, implicating Che1 in the reduced swimming speed. These results suggest that it is the combination of reduced swimming speed while maintaining the ability to reverse that caused the erratic swimming pattern of the Δ*che4* mutant strain (Fig. 3A). Together, the data confirm the role of Che1 and Che4 in regulating the motility patterns of swimming cells and in chemotaxis. They also provide further support to the hypothesis of a functional signaling interaction between Che1 and Che4.

The aerotactic advantage of coordinated regulation of swimming speed and reversals. We wondered what could be the advantage for *A. brasilense* cells in using two distinct chemotaxis signaling systems regulating two different parameters of swimming motility to modulate taxis responses. Che1, via signaling through CheY1 (6) regulates transient increases in swimming speed. Che4, via signaling through CheY4, controls reversals, as shown here. We hypothesized that a transient increase in the swimming speed that would accompany a suppression of swimming reversals during response to an attractant would enhance the net movement of cells in this gradient. To test this hypothesis, we compared aerotaxis in a spatial gradient assay of the wild type strain with

that of its Δ*cheY1* and Δ*cheY4* mutant derivatives in a time course experiment (Fig. 5). As expected, the Δ*cheY4* strain did not form an aerotactic band although cells were fully motile. The wild type strain started forming an aerotactic band after 90 seconds and a stable aerotactic band was formed by 150 sec. The initiation of the aerotactic band took almost twice as much time for the Δ*cheY1* strain, which formed a stable aerotactic band at 300 sec post-inoculation in the capillary tubes. This delay in the formation of the aerotactic band by the Δ*cheY1* cells relative to the wild type strain was consistent. These results suggest that the control of swimming speed by Che1 enhances the response of *A. brasilense* cells to a gradient of a major attractant, oxygen.

Che4 control plant association. The major role of Che4 in controlling chemotaxis and the swimming pattern suggested it should also play a significant role in the ability of cells to colonize the roots of cereals, such as wheat, a common host plant for *A. brasilense*. When inoculated alone to sterile wheat plants, the wild type and its Δ*che4* mutant derivative were able to colonize sterile wheat roots (Fig. 6A), but the mutants did so at a relatively reduced level compared to the wild type. Given that chemotaxis provides bacteria with a competitive advantage, we hypothesized that the colonization defects of the mutants would become apparent in competition experiments against the wild type strain and thus compared the competitive index of the Δ*che4* mutant when inoculated at a 1:1 ratio with the wild type strain (Fig. 6B). The competition experiments showed that lack of *che4* significantly impaired the competitive ability of the strains for colonization of the wheat root surfaces, confirming the major role of this pathway in the lifestyle of *A. brasilense* in the rhizosphere.

DISCUSSION

Experimental evidence shows that Che4 signaling controls swimming reversals in *A. brasilense* and that it is the major pathway for all taxis responses in this species. As expected from its major function in regulating chemotaxis responses, Che4 is essential for competitive root surface colonization in *A. brasilense*. The *A. brasilense* Che4 pathway is orthologous to the major pathway controlling all chemotaxis responses in *S. meliloti* (27, 28) and *R. leguminosarum* (23) where this chemotaxis system is also essential for plant root colonization. Che4 is present in the genomes of all *Azospirillum* strains sequenced to date (7-9), but absent from the phylogenetically related aquatic *R. centenum* (10). In *R. centenum*, the Che1 chemotaxis system controls all chemotaxis responses (13) while its homolog in *A. brasilense* (Che1) controls swimming speed (6). Furthermore, mutations in the *A. brasilense che1* did not affect the ability to colonize the surface of wheat roots, indicating that this pathway does not contribute to the rhizosphere lifestyle of this organism (19). Lateral gene transfer (LGT) is considered a major driving force in the evolution of prokaryotes, including the acquisition of functions for adaptation to new niches (29). The *A. brasilense* Che4 pathway was previously identified as one of the functions acquired by LGT by the ancestors of *Azospirillum* spp. that were proposed to have contributed to the adaptation to the rhizosphere (10). The role for Che4 in root surface colonization characterized here is thus consistent with this hypothesis. Che4 is a representative of the F7 class of chemotaxis systems (3) that was shown to be enriched in rhizosphere bacterial communities relative to those found in soil (2). The F7 chemotaxis systems such as the *A. brasilense* Che4 may thus be advantageous in this environment.

However, the specific competitive advantage(s) that signaling via such a chemotaxis pathway provides remains to be identified.

The acquisition of Che4 by LGT in the ancestor of *Azospirillum* spp. did not cause Che1 to lose its function in chemotaxis. Indeed, our results indicate that both Che1 and Che4 have a role in the regulation of the swimming pattern of motile *A. brasilense* cells and thus chemotaxis. However, the contribution of Che1 and Che4 to this behavior is significantly different. As shown previously (6) and in the present study, Che1 controls transient increases in swimming speed while Che4 controls the probability of swimming reversals and plays a major role in all taxis responses. Our data indicate that signaling via Che4 controls most swimming reversals with Che1 modulating this behavior via direct effects on speed. This is in contrast to the role of two chemotaxis pathways in *R. sphaeroides*, a bacterial species that has been extensively studied in this respect (30). Two chemotaxis systems, named CheOp2 and CheOp3, are implicated in the control of chemotaxis in motile *R. sphaeroides* and the signaling output from both chemotaxis pathways controls stops in the rotation of flagellar motors (31, 32). Consistent with a single signaling output, inactivation of either CheOp2 or CheOp3 abolishes chemotaxis in *R. sphaeroides*. This is because both signaling pathways ultimately affect the activity of a common set of CheY response regulators that bind the flagellar motors to stop their rotation (33, 34). This is in contrast with the results obtained here for *A. brasilense* that suggest that signaling output from both Che1 and Che4, likely mediated via CheY1 (6) and CheY4, respectively, alters different parameters of flagellar motor activity. The control of chemotaxis by two Che pathways in *A. brasilense* thus illustrates a distinct strategy by which signaling input from multiple Che pathways regulates chemotaxis.

Several lines of experimental evidence also support the hypothesis of signal integration via functional interaction between Che1 and Che4. First, inactivation of *cheA4* completely suppressed reversals and it also caused the cells to swim at a reduced speed compared to the wild type strain (24, 35). Second, strains lacking CheY4 or Che4 function were significantly impaired but not null for chemotaxis unless *cheY1* or *che1*, respectively, were also deleted. The discrepancy between the swimming speed phenotype of the Δ*cheA4* and Δ*cheY4* strains indirectly supports the hypothesis of functional interaction between Che1 and Che4 because a Δ*cheA1* strain, but not a Δ*cheY1* strain also swam at a slower speed than the wild type *A. brasilense* (6). The lack of observable swimming speed defects in strains lacking CheY1 or CheY4 could either result from functional redundancy between CheY1, CheY4 and any of the 5 other CheY homologs encoded in the genome (10) or some other unidentified interactions between Che1 and Che4 proteins. The mechanism by which signaling from Che1 and Che4 is integrated to affect swimming speed and reversals remains to be elucidated but previous data suggested that chemotaxis receptors and adaptation proteins may be involved in this process (11, 35). This was also suggested for the role of Che1 and Che2 in *Rhizobium leguminosarum* bv. *viciae* chemotaxis (23) and demonstrated as an existing mechanism in *R. sphaeroides* (31, 32).

Increased swimming speed during chemotaxis provides an advantage for marine bacteria in the exploitation of transient sources of nutrients in the oceans (36). Like the ocean, the soil is a heterogeneous environment characterized by plethora of nutrient gradients that change rapidly in space and time (37). In contrast to the ocean, the soil is less limiting in many essential nutrients and as a result, it harbors abundant and diverse

461 microbial communities (38). Oxygen may be particularly limiting in the rhizosphere
462 where microbial cell densities and microbial activities are greatest (39, 40), making
463 oxygen a potential modulator of microbial activities and competition in this environment.
464 Consistent with this hypothesis, a major chemotaxis receptor for sensing oxygen and
465 other metabolism-related parameters is critical for the ability of *A. brasilense* to colonize
466 the wheat root surface (41). Results obtained here suggest that *A. brasilense* derives an
467 aerotactic advantage from increased swimming speed, which is expected to be significant
468 in the competitive environment of the rhizosphere. The additive roles of two chemotaxis
469 systems controlling distinct motility parameters illustrated here by the *A. brasilense* Che1
470 and Che4 suggest a potential benefit that the control of chemotaxis by two (or more)
471 pathways provide motile bacteria in a competitive environment. Given the ubiquitous
472 distribution of multiple chemotaxis pathways in the genomes of rhizosphere bacteria, we
473 expect this strategy to be widespread.
474

475 ***Acknowledgements***

476 This research is supported by National Science Foundation grant NSF-MCB 1330344 (to
477 GA) and the National Natural Science Foundation of China (31370108) and One
478 Hundred-Talent Plan of the Chinese Academy of Sciences (CAS) (to ZX). Any opinions,
479 findings, conclusions, or recommendations expressed in this material are those of the
480 authors and do not necessarily reflect the views of the National Science Foundation.
481

482 **References**

1. **Wadhams GH, Armitage JP.** 2004. Making sense of it all: bacterial chemotaxis. Nat Rev Mol Cell Biol **5:**1024-1037.

2. **Buchan A, Crombie B, Alexandre GM.** 2010. Temporal dynamics and genetic diversity of chemotactic-competent microbial populations in the rhizosphere. Environ Microbiol **12:**3171-3184.

3. **Wuichet K, Zhulin IB.** 2010. Origins and Diversification of a Complex Signal Transduction System in Prokaryotes. Sci Signal **3:**ra50.

4. **Porter SL, Wadhams GH, Armitage JP.** 2008. *Rhodobacter sphaeroides*: complexity in chemotactic signalling. Trends Microbiol **16:**251-260.

5. **Zhulin IB, Armitage JP.** 1993. Motility, chemokinesis, and methylation-independent chemotaxis in *Azospirillum brasilense*. J Bacteriol **175:**952-958.

6. **Bible A, Russell MH, Alexandre G.** 2012. The *Azospirillum brasilense* Che1 Chemotaxis Pathway Controls Swimming Velocity, Which Affects Transient Cell-to-Cell Clumping. J Bacteriol **194:**3343-3355.

7. **Cecagno R, Fritsch TE, Schrank IS.** 2015. The Plant Growth-Promoting Bacteria *Azospirillum amazonense*: Genomic Versatility and Phytohormone Pathway. Biomed Res **2015:**7.

8. **Wisniewski-Dyé F, Lozano L, Acosta-Cruz E, Borland S, Drogue B, Prigent-Combaret C, Rouy Z, Barbe V, Herrera AM, González V, Mavingui P.** 2012. Genome Sequence of *Azospirillum brasilense* CBG497 and Comparative Analyses of *Azospirillum* Core and Accessory Genomes provide Insight into Niche Adaptation. Genes **3:**576.

9. **Rivera D, Revale S, Molina R, Gualpa J, Puente M, Maroniche G, Paris G, Baker D, Clavijo B, McLay K, Spaepen S, Perticari A, Vazquez M, Wisniewski-Dyé F, Watkins C, Martínez-Abarca F, Vanderleyden J, Cassán F.** 2014. Complete Genome Sequence of the Model Rhizosphere Strain *Azospirillum brasilense* Az39, Successfully Applied in Agriculture. Genome Announc **2**.

10. **Wisniewski-Dyé F, Borziak K, Khalsa-Moyers G, Alexandre G, Sukharnikov LO, Wuichet K, Hurst GB, McDonald WH, Robertson JS, Barbe V, Calteau A, Rouy Z, Mangenot S, Prigent-Combaret C, Normand P, Boyer M, Siguier P, Dessaux Y, Elmerich C, Condemine G, Krishnen G, Kennedy I, Paterson AH, González V, Mavingui P, Zhulin IB.** 2011. *Azospirillum* Genomes Reveal Transition of Bacteria from Aquatic to Terrestrial Environments. PLoS Genet **7:**e1002430.

11. **Stephens BB, Loar SN, Alexandre G.** 2006. Role of CheB and CheR in the Complex Chemotactic and Aerotactic Pathway of *Azospirillum brasilense*. J Bacteriol **188:**4759-4768.

12. **Bible AN, Khalsa-Moyers GK, Mukherjee T, Green CS, Mishra P, Purcell A, Aksenova A, Hurst GB, Alexandre G.** 2015. Metabolic adaptations of *Azospirillum brasilense* to oxygen stress by cell-cell clumping and flocculation. Appl Environ Microbiol **81**:8346-8357.

13. **Jiang ZY, Gest H, Bauer CE.** 1997. Chemosensory and photosensory perception in purple photosynthetic bacteria utilize common signal transduction components. J Bacteriol **179:**5720-5727.

14. **Hauwaerts D, Alexandre G, Das SK, Vanderleyden J, Zhulin IB.** 2002. A major chemotaxis gene cluster in *Azospirillum brasilense* and relationships between chemotaxis operons in α-proteobacteria. FEMS Microbiol Lett **208:**61-67.

15. **Vanstockem M, Michiels K, Vanderleyden J, Van Gool AP.** 1987. Transposon Mutagenesis of *Azospirillum brasilense* and *Azospirillum lipoferum*: Physical Analysis of Tn5 and Tn5-Mob Insertion Mutants. Appl Environ Microbiol **53:**410-415.

16. **Higuchi R, Krummel B, Saiki RK.** 1988. A general method of *in vitro* preparation and specific mutagenesis of DNA fragments: study of protein and DNA interactions. Nucleic Acids Res **16:**7351-7367.

17. **Krause A, Doerfel A, Gottfert M.** 2002. Mutational and transcriptional analysis of the type III secretion system of *Bradyrhizobium japonicum*. Mol plant-microbe interact **15:**1228-1235.

18. **Alexandre G, Greer SE, Zhulin IB.** 2000. Energy Taxis Is the Dominant Behavior in *Azospirillum brasilense*. J Bacteriol **182:**6042-6048.

19. **Siuti P, Green C, Edwards AN, Doktycz MJ, Alexandre G.** 2011. The chemotaxis-like Che1 pathway has an indirect role in adhesive cell properties of *Azospirillum brasilense*. FEMS Microbiol Lett **323:**105-112.

20. **Altschul SF, Gish W, Miller W, Myers EW, Lipman DJ.** 1990. Basic local alignment search tool. J Mol Biol **215:**403-410.

21. **Mohari B, Licata NA, Kysela DT, Merritt PM, Mukhopadhay S, Brun YV, Setayeshgar S, Fuqua C.** 2015. Novel Pseudotaxis Mechanisms Improve

Migration of Straight-Swimming Bacterial Mutants Through a Porous Environment. mBio **6**.

22. **Wolfe AJ, Berg HC.** 1989. Migration of bacteria in semisolid agar. Proc Natl Acad Sci U S A **86:**6973-6977.

23. **Miller LD, Yost CK, Hynes MF, Alexandre G.** 2007. The major chemotaxis gene cluster of *Rhizobium leguminosarum* bv. *viciae* is essential for competitive nodulation. Mol Microbiol **63:**348-362.

24. **Bible AN, Stephens BB, Ortega DR, Xie Z, Alexandre G.** 2008. Function of a Chemotaxis-Like Signal Transduction Pathway in Modulating Motility, Cell Clumping, and Cell Length in the Alphaproteobacterium *Azospirillum brasilense*. J Bacteriol **190:**6365-6375.

25. **Lauga E, DiLuzio WR, Whitesides GM, Stone HA.** 2006. Swimming in Circles: Motion of Bacteria near Solid Boundaries. Biophys J **90:**400-412.

26. **Lemelle L, Palierne J-F, Chatre E, Place C.** 2010. Counterclockwise Circular Motion of Bacteria Swimming at the Air-Liquid Interface. J Bacteriol **192:**6307-6308.

27. **Armitage JP, Schmitt R.** 1997. Bacterial chemotaxis: *Rhodobacter sphaeroides* and *Sinorhizobium meliloti* - variations on a theme? Microbiology **143:**3671-3682.

28. **Greek M, Platzer J, Sourjik V, Schmitt R.** 1995. Analysis of a chemotaxis operon in *Rhizobium meliloti*. Mol Microbiol **15:**989-1000.

29. **Koonin EV, Makarova KS, Aravind L.** 2001. Horizontal Gene Transfer in Prokaryotes: Quantification and Classification. Ann Rev Microbiol **55:**709-742.

30. **Porter SL, Wadhams GH, Armitage JP.** 2011. Signal processing in complex chemotaxis pathways. Nat Rev Microbiol **9:**153-165.

31. **Porter SL, Warren AV, Martin AC, Armitage JP.** 2002. The third chemotaxis locus of *Rhodobacter sphaeroides* is essential for chemotaxis. Mol Microbiol **46:**1081-1094.

32. **Shah DSH, Porter SL, Martin AC, Hamblin PA, Armitage JP.** 2000. Fine tuning bacterial chemotaxis: analysis of *Rhodobacter sphaeroides* behaviour under aerobic and anaerobic conditions by mutation of the major chemotaxis operons and *cheY* genes. EMBO J **19:**4601-4613.

33. **Pilizota T, Brown MT, Leake MC, Branch RW, Berry RM, Armitage JP.** 2009. A molecular brake, not a clutch, stops the *Rhodobacter sphaeroides* flagellar motor. Proc Natl Acad Sci U S A **106:**11582-11587.

34. **Porter SL, Wadhams GH, Martin AC, Byles ED, Lancaster DE, Armitage JP.** 2006. The CheYs of *Rhodobacter sphaeroides*. J Biol Chem **281:**32694-32704.

35. **Russell MH, Bible AN, Fang X, Gooding JR, Campagna SR, Gomelsky M, Alexandre G.** 2013. Integration of the Second Messenger c-di-GMP into the Chemotactic Signaling Pathway. mBio **4**.

36. **Stocker R, Seymour JR.** 2012. Ecology and Physics of Bacterial Chemotaxis in the Ocean. Microbiol Mol Biol Rev **76:**792-812.

37. **Carvalhais LC, Dennis PG, Fan B, Fedoseyenko D, Kierul K, Becker A, von Wiren N, Borriss R.** 2013. Linking Plant Nutritional Status to Plant-Microbe Interactions. PLoS ONE **8:**e68555.

38. **Philippot L, Raaijmakers JM, Lemanceau P, van der Putten WH.** 2013. Going back to the roots: the microbial ecology of the rhizosphere. Nat Rev Micro **11:**789-799.

39. **Hinsinger P, Bengough AG, Vetterlein D, Young I.** 2009. Rhizosphere: biophysics, biogeochemistry and ecological relevance. Plant Soil **321:**117-152.

40. **Flessa H.** 1994. Plant-induced changes in the redox potential of the rhizospheres of the submerged vascular macrophytes *Myriophyllum verticillatum* L. and *Ranunculus circinatus* L. Aquat Bot **47:**119-129.

41. **Greer-Phillips SE, Stephens BB, Alexandre G.** 2004. An Energy Taxis Transducer Promotes Root Colonization by *Azospirillum brasilense*. J Bacteriol **186:**6595-6604.

42. **Simon R, Priefer U, Puhler A.** 1983. A Broad Host Range Mobilization System for *In Vivo* Genetic Engineering: Transposon Mutagenesis in Gram Negative Bacteria. Nat Biotech **1:**784-791.

43. **Keen NT, Tamaki S, Kobayashi D, Trollinger D.** 1988. Improved broad-host-range plasmids for DNA cloning in Gram-negative bacteria. Gene **70:**191-197.

44. **Dennis JJ, Zylstra GJ.** 1998. Plasposons: Modular Self-Cloning Minitransposon Derivatives for Rapid Genetic Analysis of Gram-Negative Bacterial Genomes. Appl Environ Microbiol **64:**2710-2715.

45. **Töpfer R, Schell J, Steinbiss HH.** 1988. Versatile cloning vectors for transient gene expression and direct gene transfer in plant cells. Nucleic Acids Res **16:** 8725.

Table 1. Strains and plasmids used in this study.

Strain or plasmid	Genotype, relevant characteristics	Reference or Source
Strains		
Azospirillum brasilense		
Wild type	Wild type strain (Sp7)	ATCC29145
AB101	Δ(*cheA1*)::*gusA-Km* (Km^r)	(24)
AB102	Δ(*cheY1*)::*Km* (Km^r)	(24)
AB103	Δ(*cheA1-cheR1*)::*Cm* (Cm^r)	(24)
AB401	Δ(*cheA4*)::Gm(Gm^r)	This work
AB402	Δ(*cheY4*)::Cm(Cm^r)	This work
AB403	Δ(*cheX4-cheD4*):: Gm(Gm^r)	This work
AB141	Δ(*cheA1*)Δ(*cheA4*) ::*gusA-Km* (Km^r), Gm(Gm^r)	This work
AB142	Δ(*cheY1*)Δ(*cheY4*) :: *Km* (Km^r), Cm(Cm^r)	This work
AB143	Δ(*che1*)Δ(*che4)* :: *Cm* (Cm^r), Gm(Gm^r)	This work
Escherichia coli		
TOP10	General cloning strain	Invitrogen
S17-1	*thi endA recA hsdR* with RP4-2Tc::Mu-Km::Tn7 integrated in chromosome	(42)
Plasmids		
pRK415	Cloning vector (Tc^r)	(43)
pRK-cheA4	pRK415 containing *cheA4*	This work
pRK-cheA4^{H54Q}	pRK415 containing *cheA4* with mutation replacing residue	This work

	H54 to Q	
pRK-*cheY4*	pRK415 containing *cheY*4	This work
pRK-*cheY4*^{D57N}	pRK415 containing *cheY4* with mutation replacing residue D57 to N	This work
pSUP202	Suicide vector, pBR325 *mob* Tc^r Amp^r Cm^r	(42)
pSUPΔ*cheA4*::Gm^r		This work
pKGmobGII	Km^r, mobilizable suicide vector	
pKGΔ*cheY4*::Cm^r		
p34S-Gm	ori ColEI Amp^r Gm^r cassette	(44)
p34S-Cm	ori ColEI Amp^r Cm^r cassette	(44)
pUC19		(45)
pSUPPOL2SCA	Derivative of pSUP202, oriT of RP4, Tc^r	(17)

Figure Legends

FIG 1 Chemotaxis gene clusters encoded within the *A. brasilense* genome.

Boxes represent open reading frames and are drawn to scale. The chemotaxis genes within each cluster were either previously characterized or identified by homology searches, as detailed in the text. RR: response regulator; HK: histidine kinase; mcp: methyl-accepting chemotaxis protein.

FIG 2 Taxis behaviors of A. *brasilense* and its *che4* mutant derivatives.

(A) Chemotaxis in the soft agar plate assay containing malate (10 mM) and ammonium chloride (18.7 mM) as carbon and nitrogen sources, respectively. The strains tested are indicated at the top of each plate. The pictures were taken after 48 h incubation at 28°C.

Representative images from at least 5 different assays are shown. (B) Aerotaxis in the spatial gradient assay. The air gradient is established by diffusion, in the direction indicated by the arrow, into the capillary tubes filled with a suspension of motile cells. The images were taken 5 minutes after placing the cells in the capillary tubes. (C) Functional complementation of the aerotaxis defects of the Δ*cheA4* mutant (C) and of the Δ*cheY4* mutant (D) in the capillary assay for aerotaxis. The photographs were taken 10 min after placing the suspension of motile cells in the capillary tubes. The plasmids carried by the strains are derivatives of the broad host range pRK415. The aerotaxis defect of the Δ*cheA4* mutant strain is rescued by expressing a wild type CheA4 but not CheA4^{H54Q} (C). Similarly, the aerotaxis defect of the Δ*cheY4* mutant strain is rescued by expressing a wild type CheY4 but not CheY4^{D57N} (D). In panels B, C and D, the number of cells was equivalent in all tubes and all strains were motile. The formation of a stable band of motile cells is indicated by *.

FIG 3 Swimming behavior of *A. brasilense* wild type and mutant derivatives lacking *che4* genes or lacking a combination of *che4* and *che1* genes.

(A) Tracks of free swimming cells of *A. brasilense* and its *che4* mutant derivatives. The tracks were obtained from digital recordings and computerized motion analysis. Representative tracks are shown. The arrows point to instances of swimming reversals. (B) Reversals were determined by computerized motion analysis, from tracks of at least 75 free-swimming cells, from 3 independent cultures. The results shown are the average numbers of swimming reversals per second for each strain analyzed, with standard

deviation. Statistically different values compared to the wild type strain (*t*-test; $p<0.05$) are indicated by *. The probability of reversals of the Δ*cheA1*, Δ*cheY1* and Δ*che1* mutant strains under similar conditions were previously published (24) and corresponded to 0.41 ± 0.1 reversal/s, 0.37 ± 0.04 reversal/s and 0.46 ± 0.05 reversal/s, respectively. (C) Tracks of free swimming cells of *A. brasilense* and its derivatives lacking both *che1* and *che4* genes. The tracks were obtained from digital recordings and computerized motion analysis (CellTrack). Representative tracks are shown. The arrows point to instances of swimming reversals.

FIG 4 Swimming speed of free-swimming cells of *A. brasilense* wild type and its mutant derivatives lacking *che4* genes or lacking a combination of *che4* and *che1* genes.

The values showed are averages of swimming speed determined by motion tracking of at least 75 cells, from three independent cultures, with standard deviation. Statistically different values compared to the wild type strain (*t*-test; $p<0.05$) are indicated by *. The swimming speeds of the Δ*cheA1*, Δ*cheY1* and Δ*che1* mutant strains under similar conditions were previously published (35) and corresponded to 22 ± 1 µm/s, 31 ± 3 µm/s and 28 ± 2 µm/s, respectively.

FIG 5 Time course of aerotactic band formation in *A. brasilense* wild type, its Δ*cheY1* and its Δ*cheY4* mutant derivatives.

Cell suspensions adjusted to equivalent numbers were placed in the capillary tubes and recording, shown at the upper left of each panel, was started immediately (t=0). All cells were motile throughout the experiments. Representative images are shown.

FIG 6 Role of Che4 in the *A. brasilense* root surface colonization of wheat.

(A) The colonization index was determined from *A. brasilense* and its Δ*che4* mutant derivative inoculated alone to sterile wheat plantlets and was calculated as Log_{10} (strain output/strain input), where the number of CFU extracted from roots after incubation is normalized to the CFU measured in the inoculated input. The dots represent the colonization index for a set of four plants (one growth chamber) inoculated with the strain indicated, horizontal bars represent the mean and the vertical lines are the standard deviation. The broken gray horizontal line represents a colonization index of 1, indicating that all inoculated cells are recovered from the plant root surface. The index is > 1 for Sp7 likely because of growth on the roots. The colonization index of the wild type and the Δ*che4* were statistically significant (*t*-test; $p<0.0001$). (B) The competitive index was determined as the ratio of the mutant to the wild type recovered from roots after being inoculated at a 1:1 ratio (mutant/wild type) and calculated as Log_{10} (mutant output/wild-type output)/(mutant input/wild-type input). The dots represent the competitive index for four plants (one growth chamber) inoculated with the strains indicated at a 1:1 ratio. The horizontal bars represent the mean and the vertical lines, the standard deviation. The broken line represents a competitive index of 1, corresponding to strains equally competitive for root surface colonization.

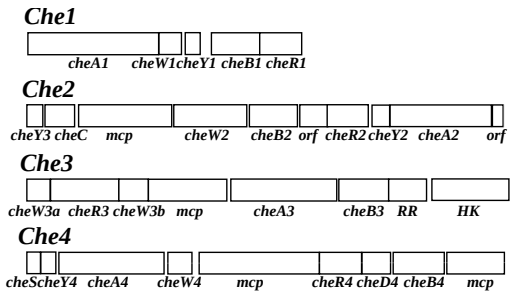

Fig. 1

Journal of Bacteriology

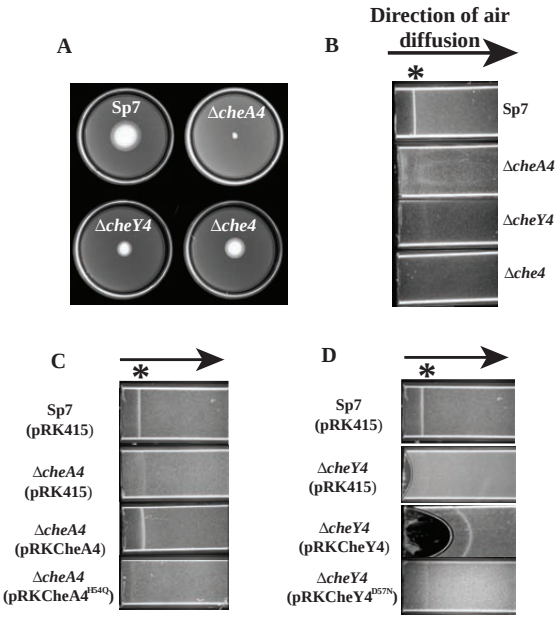

Fig. 2

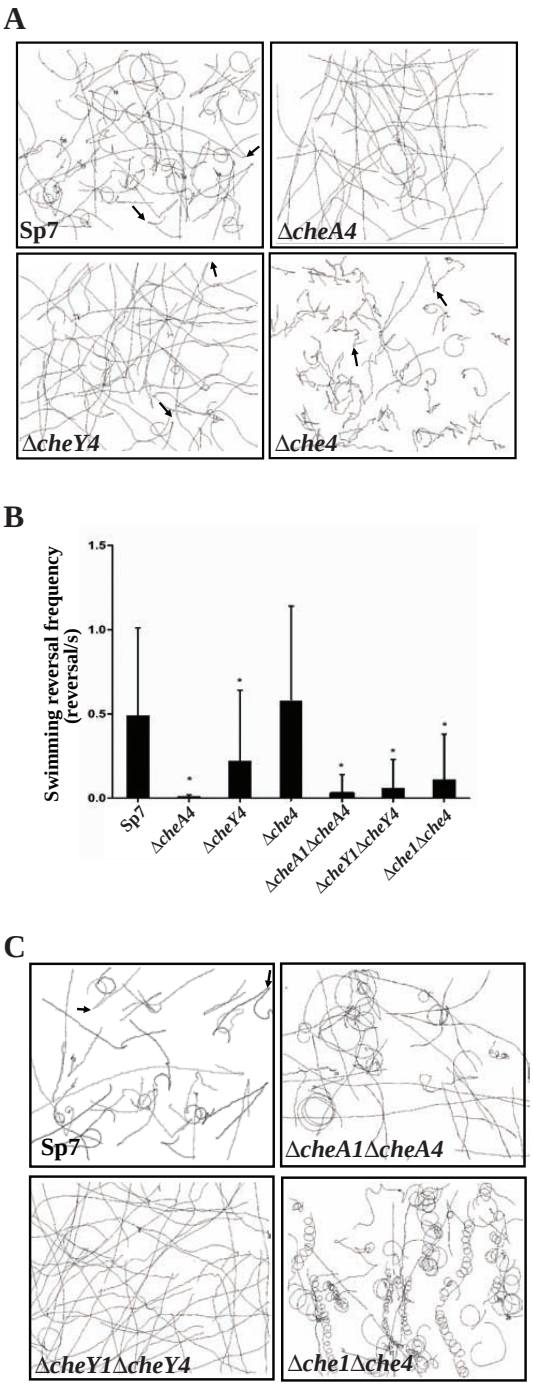

Fig. 3

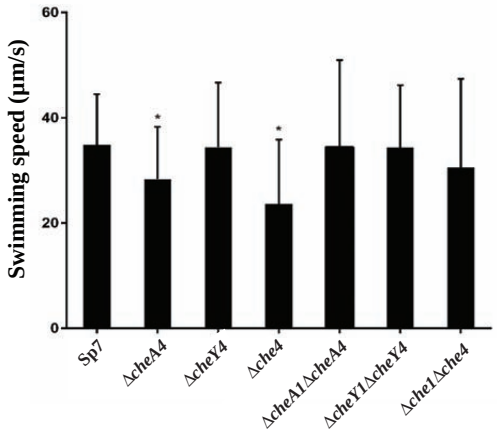

Fig. 4

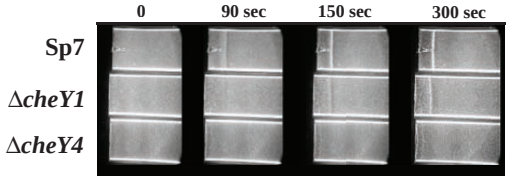

Fig. 5

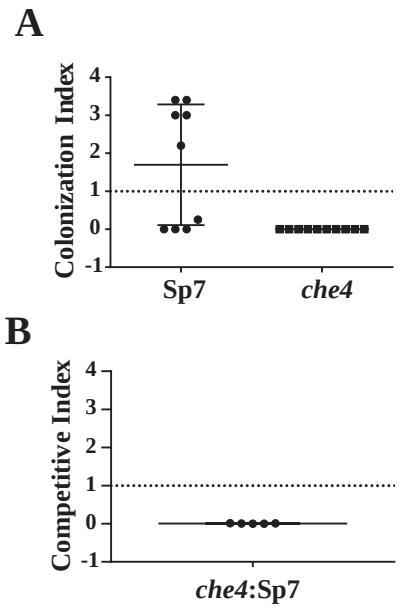

Fig. 6